GEOPHYSICAL RESEARCH LETTERS, VOL. 35, L03818, DOI:10.1029/2007GL031075, 2008

Supplementary material to article: Cloud forming potential of secondary organic aerosol under near atmospheric conditions

J. Duplissy,[1] M. Gysel,[1] M. R. Alfarra,[1] J. Dommen,[1] A. Metzger,[1]
A.S.H. Prevot,[1] E. Weingartner,[1] A. Laaksonen,[2,3] T. Raatikainen,[3] N. Good,[4]
S. F. Turner,[4] G. McFiggans,[4] and U. Baltensperger[1]

1. Instrumentation

1.1. AMS

An Aerodyne quadrupole aerosol mass spectrometer (Q-AMS) was used to provide on-line, quantitative measurements of the chemical composition and mass size distributions of the non-refractory fraction of the SOA particles at a temporal resolution of two minutes. In brief, the AMS utilizes an aerodynamic lens [*Zhang et al.*, 2004, 2002] to produce a collimated particle beam that impacts on a porous tungsten surface heated typically to 600°C under high vacuum ($\sim 10^{-8}$ Torr), causing the non-refractory fraction of the particles to flash vaporize. The vapor plume is immediately ionized using a 70 eV electron impact (EI) ionization source, and a quadrupole mass spectrometer (QMA 410, Balzers, Liechtenstein) is used to analyze the resultant ions with unit mass-to-charge (m/z) resolution. More detailed descriptions of the AMS measurement principles and various calibrations [*Jayne et al.*, 2000], its modes of operation [*Jimenez et al.*, 2003] and data processing and analysis [*Allan et al.*, 2004, 2003] are available in other publications.

1.2. HTDMA

A hygroscopicity tandem differential mobility analyzer (HTDMA) was used to measure diameter growth factors GF_D at well defined relative humidity (RH) compared to the particle dry size. A sketch of the instrument used in this study is shown in Figure S1, and a detailed description of the measurement principle is given in *Weingartner et al.* [2002] and *Gysel et al.* [2002]. The chamber aerosol is brought to charge equilibrium and dried before selecting a monodisperse size cut in DMA1. These particles are in a first step humidified to 70% RH at 24°C and then conditioned to 95% RH (10–14 s) by cooling to 19°C upon arrival in the temperature controlled box. The equilibrium diameter is measured with a second DMA operated at 95% RH. Great care was taken to maintain constant temperature in the two boxes system ($\Delta T < 0.1$°C) and the RH in DMA2 was determined by means of an accurate dewpoint sensor measurement. GF_D values are obtained with an inversion algorithm taking the full HTDMA transfer function into account [*Gysel et al.*, in preparation]. Measurement uncertainties mainly arise from RH with an accuracy of ±1%, while GF_D are highly precise and have an accuracy of ±0.02. GF_D measured at RH between 94 and 96% in DMA2 were corrected to the nominal RH of 95% using the approach discussed below for the extrapolation of growth curves.

The GF_D reported in Figure 1 originate from different dry sizes (D_0=30–150 nm). However, they are not separately marked since there is no systematic trend of GF_D with dry size selected at any time, also seen in Figure S2, as is to be expected for a mono-modal SOA aerosol originating from a single nucleation burst followed by condensational growth. The dry sizes selected with the HTDMA (30 nm, 50 nm, ...) were chosen to follow the modal diameter of the number size distribution as measured by the SMPS.

1.3. CCNC

A cloud condensation nucleus counter (CCNC) was used to measure the number concentration of activated droplets following exposure of the sample to a particular supersaturation. The CCNC used for this work was produced by Droplet Measurement Technologies, and is reviewed in *Roberts and Nenes* [2005]. The CCNC was calibrated using nebulized ammonium sulfate (Fluka, purity>99.5%) and sodium chloride (Fluka, purity>99.5%) test aerosols. The test aerosol was nebulized, dried and then sized using a DMA (TSI model 3080). The (quasi) monodisperse aerosol was then split between the CCNC and a condensation particle counter (CPC). A series of sizes were selected for each test aerosol with theoretical critical supersaturations covering the experimental supersaturation setting range, with a focus on supersaturations below 0.5% where most of the SOA measurements were made. The supersaturation settings of the CCNC required to give 50% activation of each size of test salt were calibrated by comparison with theoretical critical supersaturations calculated from the Aerosol Diameter Dependent Equilibrium Model (ADDEM) [*Topping et al.*, 2005].

During chamber experiments the CCNC was used in two ways: taking a polydisperse sample directly from the aerosol chamber, and taking a monodisperse sample downstream of a DMA. For a polydisperse sample, the size distribution of particles was measured separately by a scanning mobility particle sizer (TSI model 3936), allowing for calculation of activation diameter assuming that the activated fraction represented the upper 50^{th} percentile of the size distribution. For a monodisperse sample the activated fraction was calculated by comparison to the total particle number concentration measured separately by a condensation particle counter. Scanning the CCNC supersaturation enables critical supersaturation to be determined, as shown in Figure S3. The critical supersaturation is that at which exactly half of the particles activate. Figure S3 demonstrates the sensitivity of the CCNC to small changes in critical supersaturation, in this case from 0.164% to 0.154% due to photochemical ageing of the α-pinene SOA particles from hour 6 to 20.

[1]Laboratory of Atmospheric Chemistry, Paul Scherrer Institut, 5232 Villigen PSI, Switzerland.
[2]Department of Physics, University of Kuopio, P.O. Box 1627, FIN-70211, Kuopio, Finland.
[3]Finnish Meteorological Institute, P.O. Box 503, 00101 Helsinki, Finland.
[4]Centre for Atmospheric Sciences, University of Manchester, PO Box 88, Manchester, M60 1QD, United Kingdom.

0094-8276/08/$5.00

2. Theory of Hygroscopic Growth

The equilibrium relative humidity RH over a solution droplet is described by the Köhler equation [*Köhler*, 1921; *McFiggans et al.*, 2006]

$$RH = a_w S_k = a_w \exp\left(\frac{4\sigma_{sol} v_w}{RTD_p}\right) , \quad (1)$$

which is the product of water activity a_w and the Kelvin correction factor S_k, accounting for the relative vapor pressure reduction due to solutes (Raoult effect) and the relative vapor pressure increase over a curved surface (Kelvin effect), respectively. σ_{sol} is the surface tension of the solution, v_w the partial molar volume of water in solution, R the ideal gas constant, T the temperature, and D_p the droplet diameter. The equilibrium RH increases monotonically from the particles dry diameter up to the critical diameter (D_{crit}), where the maximum RH (RH_{max}>100%) is reached, before monotonically decreasing towards RH=100% for even larger diameters. A solution droplet is therefore in stable equilibrium for RH<RH_{max} but becomes unstable at the critical supersaturation (S_{crit}=RH_{max} − 1), meaning that it undergoes unlimited growth as long as the water vapor supply is sustained.

Assuming that solvent and solute volumes are additive, growth factor GF_D and water activity a_w of a particle are related by *Kreidenweis et al.* [2005]

$$\begin{aligned} GF_D &= \sqrt[3]{1 + \nu\Phi\frac{M_w\rho_s}{M_s\rho_w}\frac{a_w}{1-a_w}} \\ &= \sqrt[3]{1 + k(a_w)\frac{a_w}{1-a_w}} \quad . \end{aligned} \quad (2)$$

The molar mass of water M_w, density of water ρ_w, solute density ρ_s and solute molar mass M_s, are constant, while the number of dissociated ions ν per molecule and the molal osmotic coefficient Φ, accounting for deviations from ideal behavior, generally depend on solution concentration. A semi-empirical growth parameterization can be obtained by replacing all material constants and interaction parameters with a single parameter k (right hand side of Eq. 2), whereas, if required, the concentration dependence of dissociation and deviations from ideality is accounted for by writing $k(a_w) = c_0 + c_1 a_w + ...$ as a polynomial in a_w [*Dick et al.*, 2000]. In this study we used a constant value k=c_0. The formula to calculate the k value from a single growth factor measurement at a defined RH is obtained by combination of Eq. 1 and 2:

$$k\left(a_w = \frac{RH}{S_k}\right) = \left(GF_D^3 - 1\right)\left(\frac{S_k}{RH} - 1\right) . \quad (3)$$

Note that Eq. 3 is equivalent to Eq. 4 in *Gysel et al.* [2004] and to the 'k-Köhler theory' described in *Petters and Kreidenweis* [2007]. For high RH Eq. 3 is also equivalent to the parameterization used by *Wex et al.* [2007], whereas minor differences at low RH arise from using Taylor series expansions. In the Kelvin correction factor S_k the solution surface tension and the partial molar volume of water are approximated by the surface tension and molar volume of pure water, which has little (<10%) effect on the k values calculated with Eq. 3. The water activity dependence of k can be obtained by growth factor measurements at different RH (Figure S2). After determination of $k(a_w)$ from HTDMA measurements at subsaturated RH, a prediction of the critical supersaturation is derived by inserting $k(a_w)$ into Eq. 1 and determining RH_{max} [*Kreidenweis et al.*, 2005]. Such predictions of S_{crit} from HTDMA data are most sensitive to the surface tension used in Eq. 1 and moderately sensitive to uncertainties in extrapolating k from a_w<0.95 towards a_w∼1 (RH supersaturated region). Figure S2 shows growth factor measurements over a wide RH range, so-called humidograms. The SOA particles exhibit water uptake at RH as low as 30%, and growth factors increase gradually with increasing RH without a deliquescence transition. The fact to be highlighted is that Köhler curves calculated with Eq. 1 and constant k describe the growth behavior very well, implying that the product $\nu\Phi$ is virtually constant over a wide RH range. Such behavior cannot necessarily be expected, but if found in the RH range below 95% one would also expect that k does not substantially change at RH above 95%. Therefore S_{crit} predictions for α-pinene SOA (and trimethylbenzene SOA, see below) can be made from a single GF_D measurement at 95% RH with small uncertainties from extrapolating k to higher a_w, leaving the surface tension as the only major uncertainty.

For a constant k the Köhler equation becomes

$$RH = a_w \exp\left(\frac{4\sigma_{sol} v_w}{RTD_0\sqrt[3]{1 + k\frac{a_w}{1-a_w}}}\right) , \quad (4)$$

and the water activity at critical supersaturation fulfils

$$\frac{\partial}{\partial a_w}\left(a_w \exp\left(\frac{4\sigma_{sol} v_w}{RTD_0\sqrt[3]{1 + k\frac{a_w}{1-a_w}}}\right)\right) = 0 . \quad (5)$$

Solving Eq. 5 for a_w and inserting the critical water activity in Eq. 4 delivers RH_{max} and thus $S_{crit}(k, D_0)$ corresponding to a given k and dry diameter D_0. The k value corresponding to a S_{crit} measured for particles of dry size D_0 can be found by variation of k until the measured S_{crit} is matched. The purpose of such an extensive calculation of k values from measured S_{crit} is to disentangle the effects of particle dry size and hygroscopicity for a series of CCN measurements with variable dry size and changing particle properties. The magnitude of k values derived from S_{crit} strongly depends on the surface tension used in Eqs. 4 and 5, however, trends in k reflect the trend of hygroscopicity under the proviso that the actual solution surface tension at D_{crit} remains constant in time. Trends of CCN derived k values assuming surface tension of pure water are shown in Figures 2 and S5. It is particularly well seen in Figure S5 that the CCN derived k values do not vary with selecting different monodisperse size cuts, fully in agreement with the HTDMA findings. This is another strong indication that the SOA particles obey standard Köhler theory.

Figure S4 shows that the predictions of S_{crit} are much more sensitive to the assumptions on the surface tension than on uncertainties of the k value. From the results shown in Figure S2 it is to be expected that the k value at ∼100% RH most likely deviates less than 25% from the k value measured at 95% RH. Therefore we can conclude from the above closure between HTDMA and CCNC that the α-pinene SOA behavior can be described with standard Köhler theory and that α-pinene SOA is neither likely to alter the surface tension of a solution droplet more than 10% at critical supersaturation (Figure S4).

3. Thermodynamic Properties of the Aerosol Material

Eq. (1) can be used to model both the $GF_D(RH)$ and S_{crit}, provided that the molar volume and the concentration dependence of activity coefficient of water and surface

tension of the aerosol substance are known, whereas in the case of substances that reduce the surface tension of water strongly the so called surface partitioning effect [*Sorjamaa et al.*, 2004; *Sorjamaa and Laaksonen*, 2006] has to be taken into account too. In order to study the thermodynamic properties of the produced aerosols relevant for hygroscopic growth and CCN activation, we employed a model substance whose properties were altered until the observed GF_D and S_{crit} were reproduced using Eq. 1 including partitioning effect. We used the well-known van Laar [*Prausnitz et al.*, 1999] equation to describe the activity coefficient, and the Szyskowski equation [*Sorjamaa and Laaksonen*, 2006] or a simple linear relationship to model the surface tension of strongly or weakly surface active substances, respectively. The two equations describing the activity coefficient and surface tension both have two adjustable parameters, so taking account of the molar volume, we have altogether five parameters that can be adjusted within some limits to model the hygroscopicity and critical supersaturation.

The thermodynamic parameters were fitted to experimental GF_D data (data from Figure S2), and the departure from the critical supersaturation of 0.16%, which is from Figure S4 at 11 hours of light on, was used as an indicator of the goodness of the model parameters. Because the organic molar volume is unknown, different values starting from 135 cm^3/mol were tested (with an organic density [*Alfarra et al.*, 2006] of 1.3 g/cm^3 this corresponds to a molar weight of about 175 g/mol). For an ideal aqueous solution (i.e. assuming unit activity coefficients and surface tension equal to that of pure water), the best molar volume to reproduce the GF_D data is close to the 135 cm^3/mol. This ideal model predicts somewhat lower critical supersaturation (0.15%) compared to the measured value. To predict the correct S_{crit} for a molar volume of 135 cm^3/mol, the modeled water activity coefficient should be increased to well above unity. (An increase in S_{crit}, can be produced also by increasing the surface tension, but we do not expect that organic substances can cause such an increase). If relatively smooth water activity coefficient is expected, this critical supersaturation can not be predicted by the thermodynamic model.

All other factors remaining the same, a larger molar volume leads to lower growth factors and higher critical supersaturation. If the molar volume is 155 cm^3/mol, an ideal solution model predicts the correct 0.16% critical supersaturation. The GF_D, however, are lower than the measured values. In this case, the growth factors are correctly predicted when water activity coefficients are lowered below unity. This decreases S_{crit}, which can be compensated by increasing organic volume. If the molar volume is increased to about 160 cm^3/mol the measured data can be explained by nearly ideal organics, which have a small effect on water activity coefficient and surface tension (nearly linear decrease of surface tension as a function of mole fraction). Above 170 cm^3/mol, we were not able to reproduce both $GF_D(RH)$ and S_{crit}, well without resorting to rather unreasonable surface tension and water activity coefficient models. Summarizing our modeling exercise, the best fit to the data is obtained with a compound which has a molar volume close to 160 cm^3/mol and which has nearly linear influence with concentration on both water activity coefficient and surface tension of the aqueous solution. It can be shown that for such substances, the semi-empirical k-model assuming surface tension of pure water as discussed above predicts critical supersaturations quite well. However, our calculations indicate that this is not necessarily the case for systems with less linear dependence of water activity coefficient and surface tension on concentration. Furthermore, it is possible that with strongly surface active substances, the k-model would predict correct S_{crit} but incorrect D_{crit}, the latter of which is usually not measured. Such potential discrepancies in k-model application warrant further attention, but do not affect the reconciliation of sub- and supersaturated behavior in the current work.

References

Alfarra, M. R., D. Paulsen, M. Gysel, A. A. Garforth, J. Dommen, A. S. H. Prévôt, D. R. Worsnop, U. Baltensperger, and H. Coe (2006), A mass spectrometric study of secondary organic aerosols formed from the photooxidation of anthropogenic and biogenic precursors in a reaction chamber, *Atmos. Chem. Phys.*, *6*(12), 5279–5293.

Allan, J. D., et al. (2004), A generalised method for the extraction of chemically resolved mass spectra from aerodyne aerosol mass spectrometer data, *J. Aerosol Sci.*, *35*(7), 909–922.

Allan, J. D., et al. (2003), Quantitative sampling using an aerodyne aerosol mass spectrometer 2. Measurements of fine particulate chemical composition in two U.K. cities, *J. Geophys. Res.*, *108*(D3), 4091, doi:10.1029/2002JD002359.

Dick, W. D., P. Saxena, and P. H. McMurry (2000), Estimation of water uptake by organic compounds in submicron aerosols measured during the southeastern aerosol and visibility study, *J. Geophys. Res.*, *105*(D1), 1471–1479.

Gysel, M., E. Weingartner, and U. Baltensperger (2002), Hygroscopicity of aerosol particles at low temperatures. 2. Theoretical and experimental hygroscopic properties of laboratory generated aerosols, *Environ. Sci. Technol.*, *36*(1), 63–68.

Gysel, M., S. Nyeki, D. Paulsen, E. Weingartner, U. Baltensperger, I. Galambos, and G. Kiss (2004), Hygroscopic properties of water-soluble matter and humic-like organics in atmospheric fine aerosol, *Atmos. Chem. Phys.*, *4*(1), 35–50.

Jayne, J. T., D. C. Leard, X. F. Zhang, P. Davidovits, K. A. Smith, C. E. Kolb, and D. R. Worsnop (2000), Development of an aerosol mass spectrometer for size and composition analysis of submicron particles, *Aerosol Sci. Technol.*, *33*(1-2), 49–70.

Jimenez, J. L., et al. (2003), Ambient aerosol sampling using the aerodyne aerosol mass spectrometer, *J. Geophys. Res.*, *108*(D7), 8425, doi:10.1029/2001JD001213.

Köhler, H. (1921), Zur Kondensation des Wassers in der Atmosphre, *Meteorol. Z.*, *38*(1), 168–171.

Kreidenweis, S. M., K. Koehler, P. J. DeMott, A. J. Prenni, C. Carrico, and B. Ervens (2005), Water activity and activation diameters from hygroscopicity data - Part I: Theory and application to inorganic salts, *Atmos. Chem. Phys.*, *5*(5), 1357–1370.

McFiggans, G., et al. (2006), The effect of physical and chemical aerosol properties on warm cloud droplet activation, *Atmos. Chem. Phys.*, *6*(9), 2593–2649.

Petters, M. D., and S. M. Kreidenweis (2007), A single parameter representation of hygroscopic growth and cloud condensation nucleus activity, *Atmos. Chem. Phys.*, *7*(8), 1961–1971.

Prausnitz, J., R. Lichtenthaler, and E. Azevedo (1999), *Molecular thermodynamics of fluid-phase equilibria*, Englewood Cliffs, N.J. Prentice-Hall.

Roberts, G. C., and A. Nenes (2005), A continuous-flow streamwise thermal-gradient ccn chamber for atmospheric measurements, *Aerosol Sci. Technol.*, *39*(3), 206–221.

Sorjamaa, R., and A. Laaksonen (2006), The influence of surfactant properties on critical supersaturations of cloud condensation nuclei, *J. Aerosol Sci.*, *37*(12), 1730–1736.

Sorjamaa, R., B. Svenningsson, T. Raatikainen, S. Henning, M. Bilde, and A. Laaksonen (2004), The role of surfactants in Köhler theory reconsidered, *Atmos. Chem. Phys.*, *4*(8), 2107–2117.

Topping, D. O., G. B. McFiggans, and H. Coe (2005), A curved multi-component aerosol hygroscopicity model framework: Part 1 - Inorganic compounds, *Atmos. Chem. Phys.*, *5*(5), 1205–1222.

Weingartner, E., M. Gysel, and U. Baltensperger (2002), Hygroscopicity of aerosol particles at low temperatures. 1. New low-temperature H-TDMA instrument: Setup and first applications, *Environ. Sci. Technol.*, *36*(1), 55–62.

Wex, H., T. Hennig, I. Salma, R. Ocskay, A. Kiselev, S. Henning, A. Massling, A. Wiedensohler, and F. Stratmann (2007), Hygroscopic growth and measured and modeled critical supersaturations of an atmospheric HULIS sample, *Geophys. Res. Lett.*, *34*(2), L17810, doi:10.1029/2007GL030185.

Zhang, R. Y., I. Suh, J. Zhao, D. Zhang, E. C. Fortner, X. X. Tie, L. T. Molina, and M. J. Molina (2004), Atmospheric new particle formation enhanced by organic acids, *Science*, *304*(5676), 1487–1490.

Zhang, X. F., K. A. Smith, D. R. Worsnop, J. Jimenez, J. T. Jayne, and C. E. Kolb (2002), A numerical characterization of particle beam collimation by an aerodynamic lens-nozzle system: Part I. An individual lens or nozzle, *Aerosol Sci. Technol.*, *36*(5), 617–631.

M. Gysel, Laboratory of Atmospheric Chemistry, Paul Scherrer Institut, 5232 Villigen PSI, Switzerland. (martin.gysel@psi.ch)

Table S1: Initial mixing ratios and SOA yields for all experiments shown in this paper.

precursor	VOC	NO	NO_2	RH	$mass_{max}$	yield
1,3,5-trimethylbenzene	135	0	65	48	8.4	0.014
α-pinene	10	0	3.8	53	5.4	0.102
α-pinene	124	31	41	49	125	0.208
α-pinene	183	48	60	52	206	0.221

'precursor': organic precursor name
'VOC': initial concentration of organic precursor; unit: ppb
'NO': initial concentration of NO; unit: ppb
'NO_2': initial concentration of NO_2; unit: ppb
'RH': relative humidity during the photo-oxidation; unit: %
'$mass_{max}$': maximum aerosol mass concentration reached during the experiment, as derived from the integrated SMPS volume assuming a particle density of 1400 kg/m^3; unit: μg/m^3
'yield': the yield (or aerosol mass fraction) is the ratio between the mass of aerosol produced to the mass of VOC reacted, calculated for the time with maximum aerosol mass concentration; unit: -

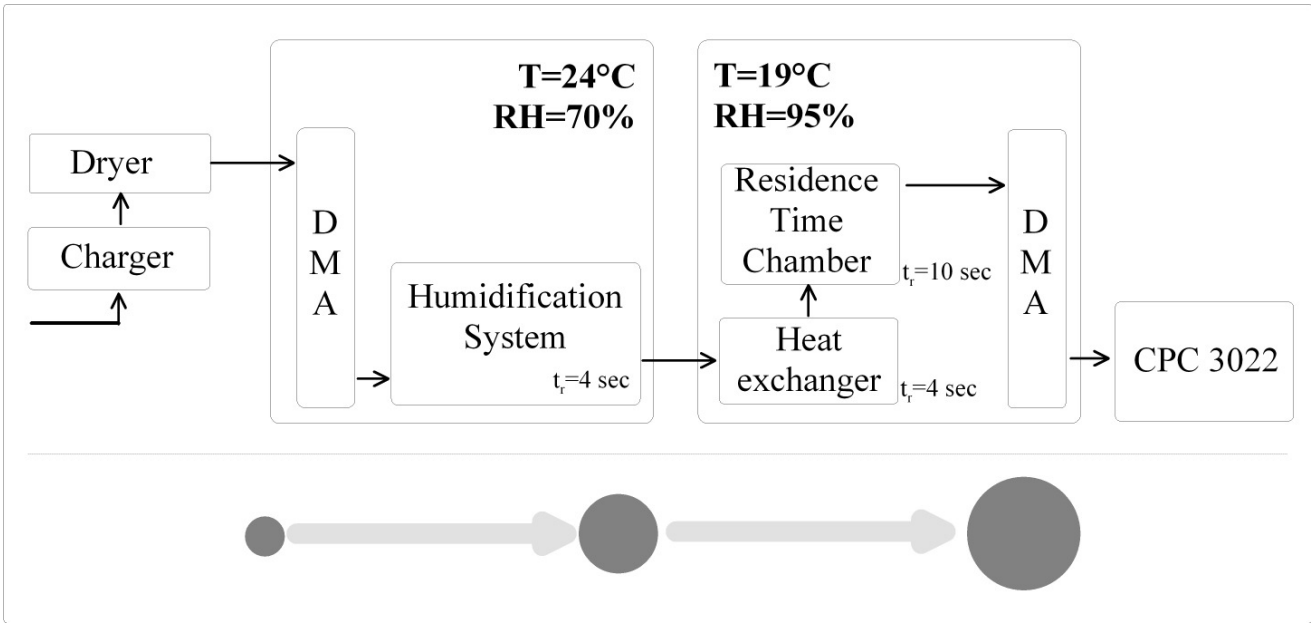

Figure S1: Schematic diagram of the HTDMA. A dry monodisperse size cut is selected in the first DMA. These particles are humidified to 70% RH at 24 °C and then conditioned to 95% RH (10-14 s) by cooling to 19 °C upon arrival in the temperature controlled box. The equilibrium diameter is then measured with the second DMA, which is operated at 95% RH. The reported growth factor is the ratio of the wet to dry sizes.

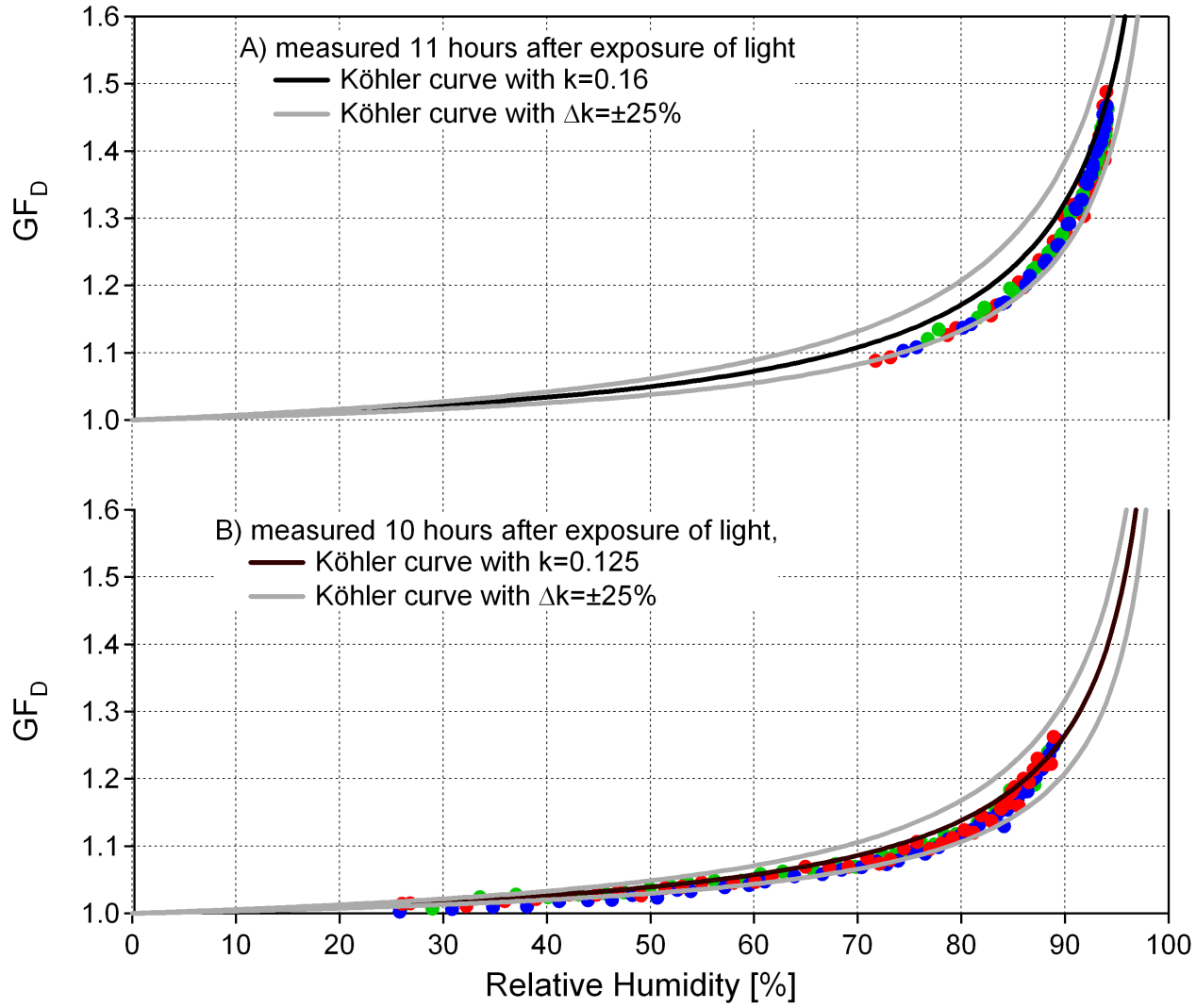

Figure S2: Measured humidograms of SOA from α-pinene. Humidograms performed during two different experiments (A and B 10 ppb α-pinene and 3.8 ppb NO_2). A) after 11 hours of irradiation while the lights were still on; B) after 10 hours of irradiation with lights turned off. Green, blue and red symbols mark the measurements for dry sizes 150, 200 and 151 nm, where the latter were obtained from doubly charged particles selected at 100 nm mobility diameter. The k values of the black Köhler curves were fitted to match the measured growth factors of 200 nm particles at RH=95%.

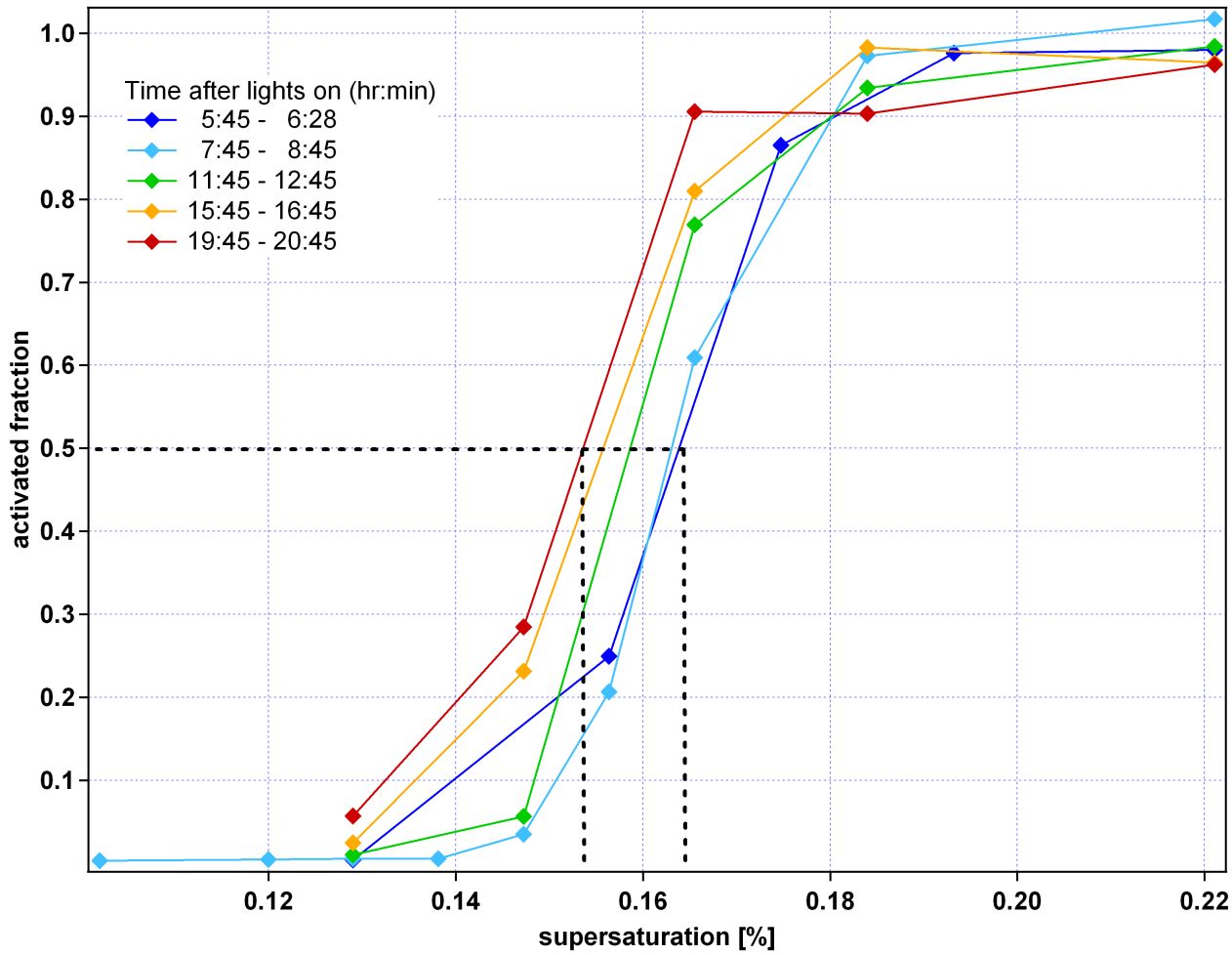

Figure S3: Activated fraction as a function of the supersaturation, from CCN measurements of 170-nm SOA particles at initially 10 ppbv α-pinene concentration. The critical supersaturation, corresponding to activated fraction of 0.5, decreased from hour 6 to 20 due to extended photo-aging.

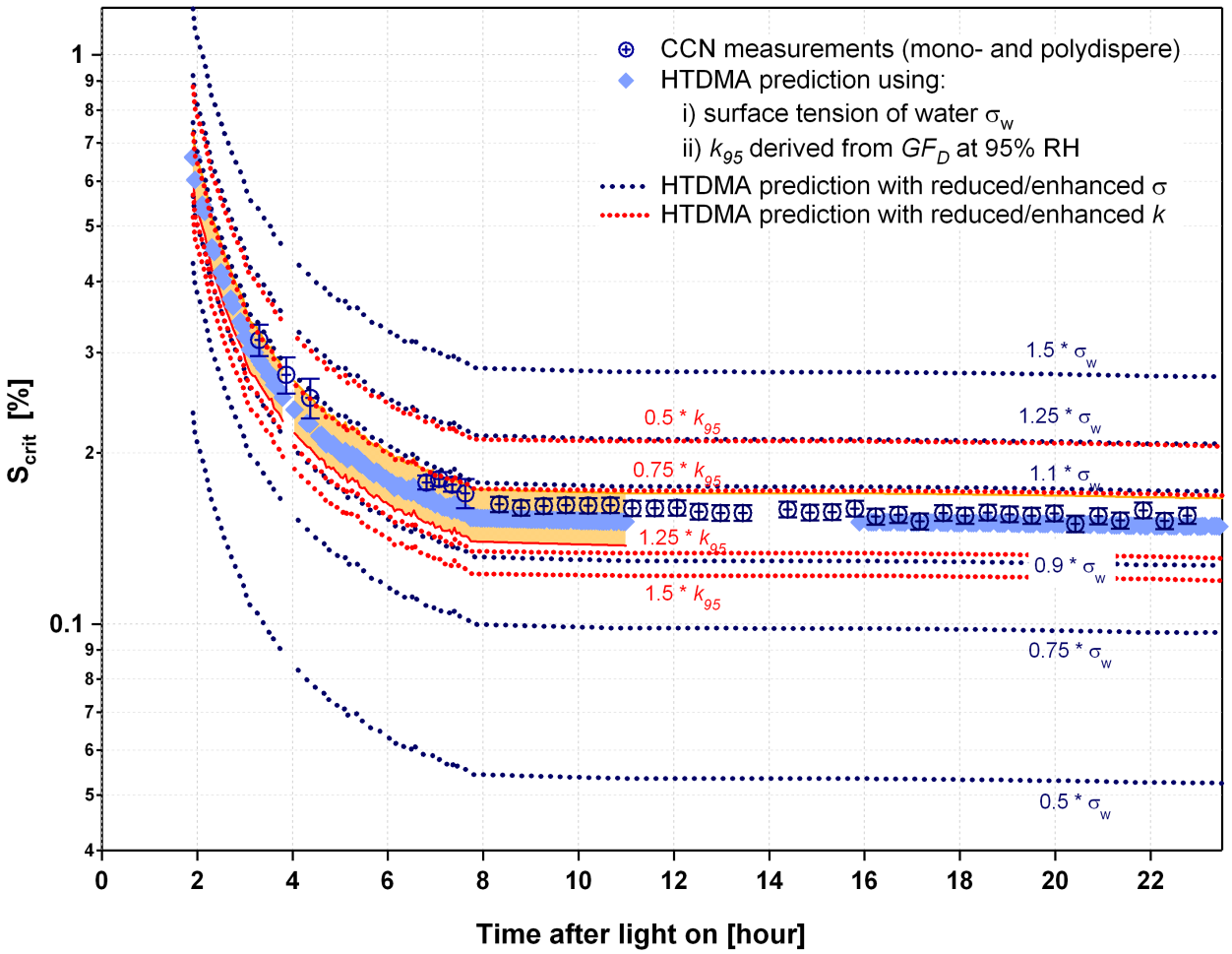

Figure S4: Sensitivity of critical supersaturation to surface tension and k value at RH=95%. CCN measurements (dark blue crossed circles) and 'base case' HTDMA predictions (light blue diamonds) as in Figure 2. Blue dotted lines show the HTDMA predictions modified with assuming 1.5, 1.25, 1.1, 0.9, 0.75, and 0.5 times surface tension of pure water. Red dotted lines show HTDMA predictions modified with using 1.5, 1.25, 0.75, and 0.5 times the k value measured at RH=95%. The sensitivity of HTDMA derived data to an RH error of ±% at 95% RH is indicated by the yellow shaded areas.

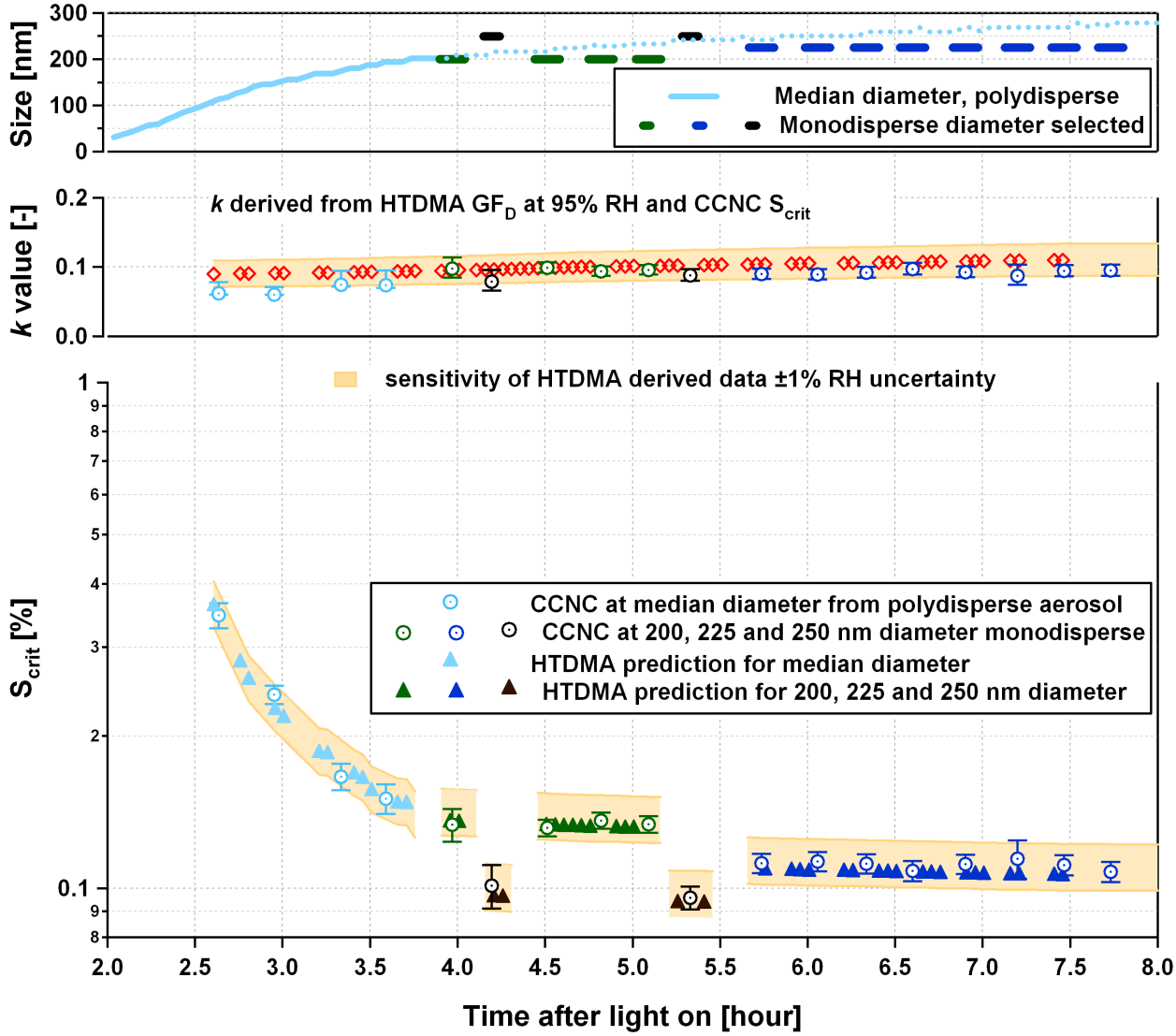

Figure S5: Closure of growth factor and critical supersaturation of SOA from 1,3,5-trimethyl benzene precursor. The same good agreement between calculated and measured critical supersaturation was found for the photo-oxidation of 1,3,5-trimethyl benzene (135 ppb and 65 ppb NO_x). The sensitivity of HTDMA derived data to an RH error of ±1% at 95% RH is indicated by the yellow shaded areas.